Fluorescent Organic Small Molecule Probes

Subjects: Chemistry, Organic

Contributor: Yufei Yang , Fucheng Gao , Yandong Wang , Hui Li , Jie Zhang , Zhiwei Sun , Yanyan Jiang

Fluorescence imaging technology provides a visual tool for medicine, showing great potential in the fields of molecular biology, cellular immunology and oncology. In recent years, organic fluorescent probes have attracted much attention in the bioanalytical field. Among various organic fluorescent probes, fluorescent organic small molecule probes (FOSMPs) have become a research hotspot due to their excellent physicochemical properties, such as good photostability, high spatial and temporal resolution, as well as excellent biocompatibility. FOSMPs have proved to be suitable for in vivo bioimaging and detection.

fluorescent organic small molecules | bioimaging | detection | recognition mechanisms | fluorescent organic nanoparticles

1. Introduction

The key substances inside the human body, including metal ions [1], biological small molecules [2][3], reactive oxygen species [4][5][6] and reactive nitrogen [7][8], are closely related to biological events, regulating physiological functions and metabolism. For instance, metal ions (e.g., Fe^{3+}, Na^{+}, Al^{3+} and Mg^{2+}) play important regulatory roles in metabolism and osmolality [9][10][11]. Biological small molecules, such as homocysteine (Hcy), cysteine (Cys) and glutathione (GSH) participate in metabolism and redox reactions [12][13][14]. The content of reactive oxygen species and reactive nitrogen reflects many pathological states, especially the development of cancer [15][16][17][18]. Therefore, monitoring the levels of these substances is helpful for understanding human health status.

With the development of in vivo imaging technology, more and more tracer techniques have been applied in biomedical research. Traditional tracing methods are usually required to remove tissues from the body, which cannot realize the real-time dynamic monitoring of the target substances. Currently, the commonly used in vivo tracer techniques include radionuclide imaging, magnetic resonance imaging (MRI), optical imaging and so on [19]. Radionuclide imaging can achieve quantitative and localization analysis of cells, but it has the shortcomings of low spatial resolution and the need of expensive equipment [20][21]. MRI with high spatial and temporal resolution enables monitoring of changes in cellular function, but this technique faces the problem of long imaging time [22]. In vivo luminescence imaging is a non-invasive technology, including bioluminescence imaging (BLI) and fluorescence imaging, mainly used to study gene expression and cell activity. Compared with BLI, the signal of fluorescence imaging is stronger and the detection accuracy is higher [23][24][25]. At present, in vivo fluorescence imaging has become a hotspot in biomedical research due to its advantages of low toxicity, high spatiotemporal resolution and utilization of an inexpensive instrument [26][27][28]. For example, fluorescent dye indocyanine green

(ICG) imaging has been used in a variety of abdominal surgery applications, such as lymph node localization, ureteral detection and tumor identification [29]. In recent years, some fluorescent probes with high specificity have also been developed and used for in vivo imaging [30][31][32].

To date, many types of fluorescent probes, such as fluorescent organics [33][34][35][36], fluorescent proteins [37], inorganic nanoparticles [38][39] and semiconductor polymer nanoparticles [40][41] have been developed and widely used in bioimaging. Fluorescent proteins can be generated by cells themselves through genetic engineering, which is convenient for in vivo imaging. However, they are hard to metabolize in the body. Inorganic nanoparticles have good spectral properties and light stability, but the biological toxicity limits their application in bioimaging. Semiconductor polymer nanoparticles have high fluorescence brightness, but slow metabolism causes them to accumulate in the liver. Comparatively, fluorescent organic small molecule probes (FOSMPs) attracted more attention because of their controllable synthesis, stable luminescence, good biocompatibility, sensitive response and high signal-to-noise ratio [42][43]. When applied to imaging, the photochemical properties of FOSMPs are generally more stable than other types of probes. Additionally, small molecules also help to achieve higher fluorophore density and spatial resolution. Therefore, a large number of FOSMPs have been designed and applied to detect substances in various matrix [44][45][46][47][48][49][50][51]. Fluorescent organic nanoparticles (FONPs), which were designed with FOSMPs as fluorophores, show the ability to build a multifunctional biosensing platform through surface functionalization and drug encapsulation [52]. A summary of the progress on the applications of FOSMPs in bioimaging and detection is of significance for the development of new diagnostic tools. There are no special reviews focusing on this field.

2. FOSMPs for Bioimaging and Detection

Fluorescence is the phenomenon that electrons return from the first singlet state to the ground state with concomitant energy release in the form of light. The characteristics of the fluorescent probes such as excitation and emission wavelength, intensity, lifetime and polarization are easily influenced by the environment conditions, thereby providing sensitive signals for the tracking and monitoring of analytes [53][54][55][56][57][58]. The structure of FOSMPs is mainly composed of three parts: the recognition group, the fluorophore, and the linking group (linker) (**Figure 1**). The recognition group endows the fluorescent probe with detection selectivity. The fluorophore provides the signal response when the probe recognizes the target. The linker connects the recognition group and the fluorophore and is not necessary for the fluorescent probe.

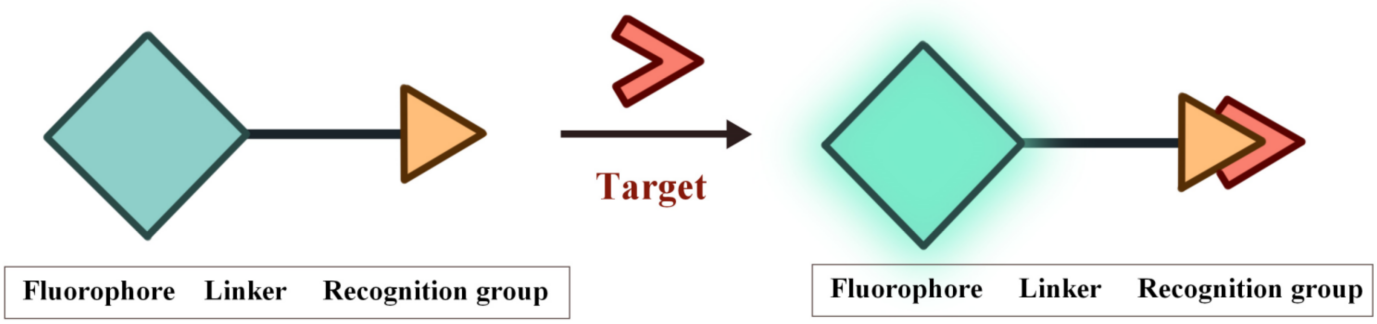

Figure 1. The structure of FOSMPs and its recognition of the target.

As shown in **Figure 2**, according to the interaction manner between FOSMPs and targets, the recognition mechanisms can be divided into five types: photo-induced electron transfer (PET), intramolecular charge transfer (ICT), fluorescence resonance energy transfer (FRET), excited state intramolecular proton transfer (ESIPT) and aggregation-induced emission (AIE). Based on these recognition mechanisms, various FOSMPs for bioimaging and detection have been developed, as listed in **Table 1**. In the following, the applications of FOSMPs in bioimaging and analysis based on these recognition mechanisms are reviewed.

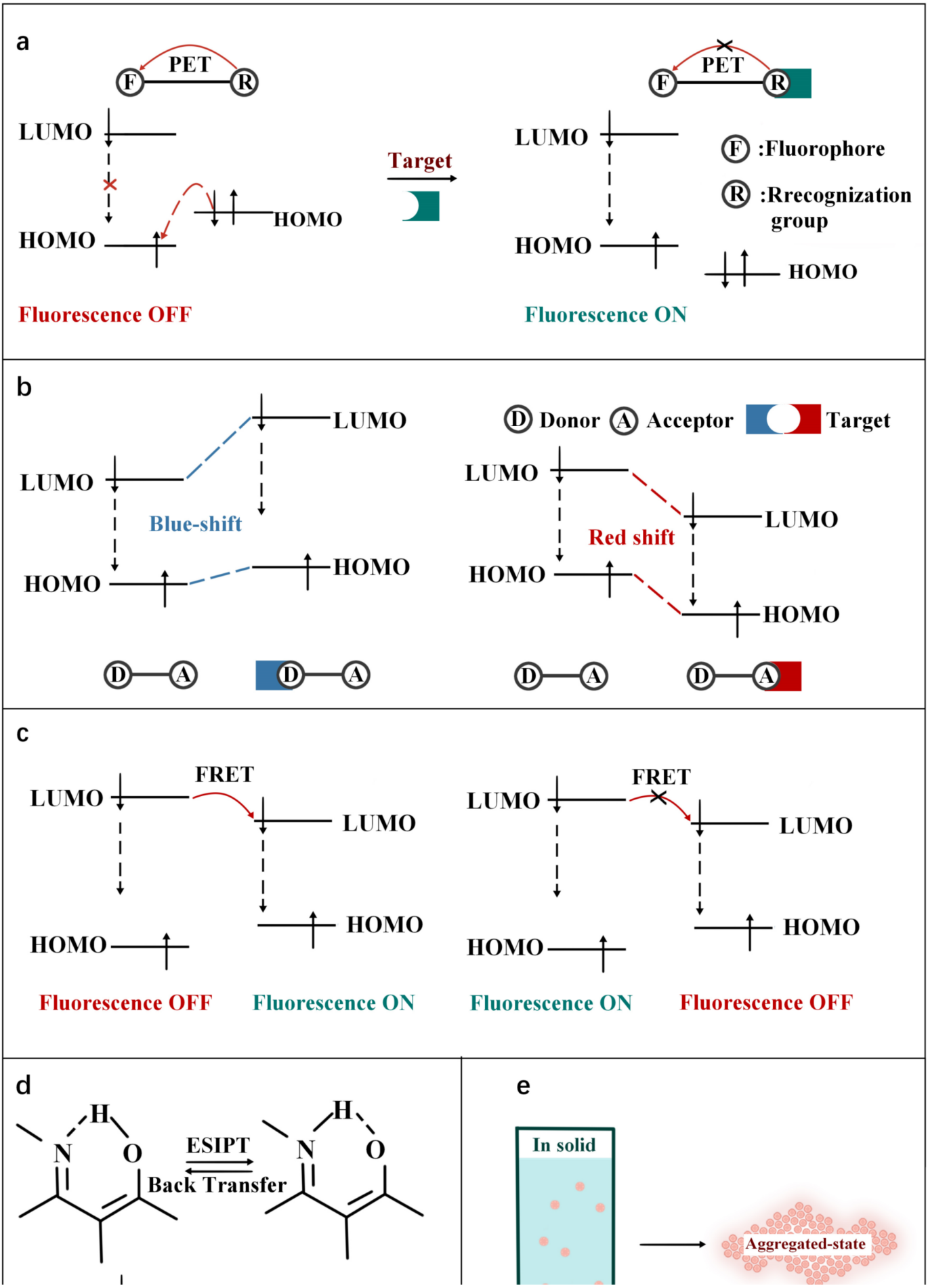
a
PET
F
R
LUMO
HOMO
Target
Fluorescence OFF
Fluorescence ON
:Fluorophore
:Rrecognization group
b
Blue-shift
Red shift
Donor
Acceptor
Target
c
FRET
Fluorescence OFF
Fluorescence ON
d
ESIPT
Back Transfer
e
In solid
Aggregated-state

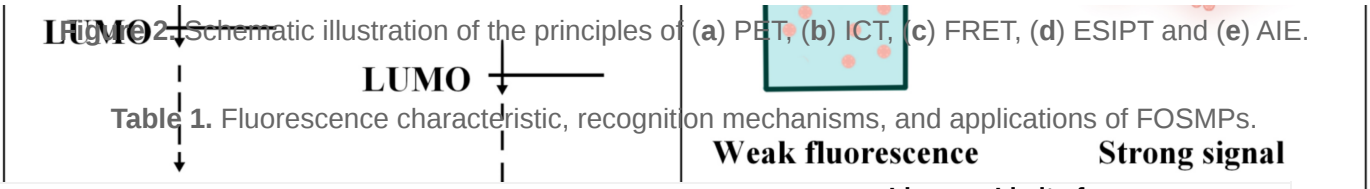

Figure 2. Schematic illustration of the principles of (**a**) PET, (**b**) ICT, (**c**) FRET, (**d**) ESIPT and (**e**) AIE.

Table 1. Fluorescence characteristic, recognition mechanisms, and applications of FOSMPs.

Probe	λex/λem (nm)	Mechanism	Analyte	Solvent System	Linear Detection Range	Limit of Detection (LOD)	Target	Ref.
Probe	500/525	PET	Cys	CH_3CN-Water-HEPES buffer	0–100 μM	3.7 × 10^{-2} μM	A375 cells	[59]
NP-S	455/551	PET	H_2S	PBS buffer-EtOH	30–300 μM	0.376 μM	Mouse liver slices	[60]
Tyro1, Tyro2	455/560	PET	Tyrosinase	Potassium phosphate buffer	-	-	B16F10 cells	[61]
NFP-G, NFP-A	440/541	PET	Formaldehyde (FA)	DMSO-PBS buffer	0–30 μM, 0–15 μM	1.2 μM, 0.18 μM	HepG-2 cells	[62]
Naphthalimide chromophore	400/502	ICT	CN^-	HEPES buffer - CH_3OH	0–15 μM	0.066 μM	HepG2 cells	[63]
DCM-β-gal	535/685	ICT	β-galactosidase (β-gal)	PBS buffer-DMSO	0–12 U/L	0.17 U/L	293T cells	[64]
DCDHF-Glu	510/613	ICT	γ-Glutamyltranspeptidase (GGT)	PBS buffer	0–40 U/L	0.0379 U/L	HepG2 cells, LO2 cells	[65]
SHC	370/540	ICT	hNQO1	PBS buffer	0–0.8 μM	0.0146 μM	HT-29 cells, MDA-MB-468 cells	[66]
AI	370/495	ICT	Hypochlorous acid (HOCl)	DMSO-PBS buffer	0–50 μM	0.84 μM	HeLa cells, Nude mice	[67]
P-$ONOO^-$	365/480	ICT	$ONOO^-$	DMSO-PBS buffer	0.429–3.0 μM	0.0104 μM	HeLa cells	[68]
SR400, SR550	400/525, 550/675	FRET	H_2S	PBS buffer	-	-	HEK293 cells	[69]

Probe	λex/λem (nm)	Mechanism	Analyte	Solvent System	Linear Detection Range	Limit of Detection (LOD)	Target	Ref.
CF	415/517	FRET	HNO	PBS buffer	0–100 μM	1.4 μM	HeLa cells	[70]
FIP-1	515/556	FRET	Fe(II)	HEPES buffer	-	-	HEK293 cells, MDAMB-231 cells	[71]
PNCy3Cy5	530/660	FRET	$OONO^-$	Phosphate buffer-DMF	0–0.7 μM	6.5×10^{-4} μM	RAW264.7	[72]
FTR-βgal	450/540	FRET	β-gal	PBS buffer-EtOH	0–5 U/L	4.11×10^{-8} U/L	Hek293 cells	[73]
PPA	400/511	ESIPT	Palladium	CH_3CN-PBS buffer	0–180 μM	0.028 μM	A549 cells	[74]
Py-GSH	488/545	ESIPT	GGT	PBS buffer	1–30 U/L	1×10^{-2} U/L	SKOV3 cells, HOSEpiC cells, Tumor-bearing mice, Human specimens	[75]
NIR-TS	550/836	ESIPT	SO_2	Water	0.5–40 μM	0.067 μM	HeLa cells, Mice	[76]
TPE-Gal	344/512	AIE	β-gal	PBS buffer	8×10^{-4}–4.8×10^{-3} U/L	3.3×10^{-4} U/L	HeLa cells, OVCAR-3 cells	[77]
TT	320/440–550	AIE	H_2O_2	DMSO-Water	-	-	RAW264.7 cells, HLF cells	[78]
QP-DNP	482/582	AIE	Hydrazine	DMSO-HEPES buffer	0–0.8 μM	0.055 μM	HeLa cells, Kunming mouse	[79]
AIE-Lyso-1	356/532	AIE/ESIPT	Esterase	DMSO–	100–	2.4 U/L	MCF-7	[80]

Compared with FOSMPs, FONPs have larger surface area, better biodegradability and greater resistance to photobleaching [83][84]. FONPs-based multifunctional biodetection platforms can be constructed through drug encapsulation and surface modification of targeting groups. Researchers briefly describes the preparation and applications of FOSMPs-based FONPs in bioimaging and detection.

Zhang et al. [85] reported a strategy to prepare FONPs by encapsulating the fluorophore C18-R in synthetic copolymer matrices. First, the copolymer aqueous solution was added to the C18-Rd THF solution under sonication. In the process of removing THF, the hydrophobic segment of the copolymer wrapped C18-R through hydrophobic interaction to form a “core-shell” structure, and finally the C18-R-PEG FONPs were obtained. CLSM

Probe	λex/λem (nm)	Mechanism	Analyte	Solvent System	Linear Detection Range	Limit of Detection (LOD)	Target	Ref.
				Water	500 U/L		cells	
Probe 1	314/446	PET/ICT	Cys	PBS buffer [86]	0.2–2.0 μM	1.4×10^{-3} μM	HeLa cells	[81]
NCQ	423/490, 544 423/490423/490, 624	Triple-emission	Cys/Hcy, GSH/H_2S, thiopheno(PhSH)	PBS buffer-acetonitrile	0–10 μM/10 μM, 0–6 μM/8 μM, 0–70 μM	0.57 μM/0.65 μM, 0.49 μM/0.52 μM, 0.34 μM	HeLa cells	[82]

luminescence and excellent biocompatibility.

1,2-distearoyl-sn-glycero-3-phosphoethanolamine-N-(polyethylene glycol) (DSPE-PEG_{2000}) is a typical package matrix that is widely used in the design of FONPs due to its good biocompatibility [87][88][89][90]. Transcription-AIE (Tat-AIE) dots prepared using DSPE-PEG_{2000} as the matrix was first reported as cell-tracing probes in 2013, showing brighter fluorescence, better fluorescence stability and cell-tracking ability than commercial quantum dot-based probes. Li et al. [88] encapsulated the fluorophore TPETPAFN by using a mixture of DSPE-PEG_{2000} and DSPE-PEG_{2000}-NH_2. Then, Tat-AIE dots were obtained by coupling AIE dots with cell penetrating peptide HIV-1 Tat. TPETPAFN has poor water solubility but is easily soluble in THF solution. The fluorescence of TPETPAFN was turned on when the THF/water volume ratio was 1:1 and the fluorescence intensity increased exponentially with the increase of the ratio of water. The fluorescence intensity of TPETPAFN showed a 70-fold enhancement at a 90% water volume fraction. The hydrodynamic size and quantum yield of the as-prepared NIR-emitting Tat-AIE dots were ~30 nm and 24%, respectively. Compared to commercial Qtracker® 655, Tat-AIE dots displayed 10-fold stronger fluorescence intensity and better long-term tracing ability. Tat-AIE dots could trace MCF-7 cells for 10–12 generations and trace C6 cells for 21 days in vivo.

References

1. Hao, J.; Yan, B. A water-stable lanthanide-functionalized MOF as a highly selective and sensitive fluorescent probe for Cd2+. Chem. Commun. 2015, 51, 7737–7740.
2. Donia, M.S.; Fischbach, M.A. Small molecules from the human microbiota. Science 2015, 349, 1254766.
3. Fukuto, J.M.; Carrington, S.J.; Tantillo, D.J.; Harrison, J.G.; Ignarro, L.J.; Freeman, B.A.; Chen, A.; Wink, D.A. Small Molecule Signaling Agents: The Integrated Chemistry and Biochemistry of Nitrogen Oxides, Oxides of Carbon, Dioxygen, Hydrogen Sulfide, and Their Derived Species. Chem. Res. Toxicol. 2012, 25, 769–793.

4. Griendling, K.K.; Touyz, R.M.; Zweier, J.L.; Dikalov, S.; Chilian, W.; Chen, Y.; Harrison, D.G.; Bhatnagar, A.; Amer, H.A.C.B. Measurement of Reactive Oxygen Species, Reactive Nitrogen Species, and Redox-Dependent Signaling in the Cardiovascular System: A Scientific Statement From the American Heart Association. Circ. Res. 2016, 119, E39–E75.
5. Jiao, X.; Li, Y.; Niu, J.; Xie, X.; Wang, X.; Tang, B. Small-Molecule Fluorescent Probes for Imaging and Detection of Reactive Oxygen, Nitrogen, and Sulfur Species in Biological Systems. Anal. Chem. 2018, 90, 533–555.
6. Kalyanaraman, B. Teaching the basics of redox biology to medical and graduate students: Oxidants, antioxidants and disease mechanisms. Redox Biol. 2013, 1, 244–257.
7. Figueira, T.R.; Barros, M.H.; Camargo, A.A.; Castilho, R.F.; Ferreira, J.C.B.; Kowaltowski, A.J.; Sluse, F.E.; Souza-Pinto, N.C.; Vercesi, A.E. Mitochondria as a Source of Reactive Oxygen and Nitrogen Species: From Molecular Mechanisms to Human Health. Antioxid. Redox Sign. 2013, 18, 2029–2074.
8. Fransen, M.; Nordgren, M.; Wang, B.; Apanasets, O. Role of peroxisomes in ROS/RNS-metabolism: Implications for human disease. Bba.-Mol. Basis Dis. 2012, 1822, 1363–1373.
9. Mehta, V.N.; Desai, M.L.; Basu, H.; Kumar Singhal, R.; Kailasa, S.K. Recent developments on fluorescent hybrid nanomaterials for metal ions sensing and bioimaging applications: A review. J. Mol. Liq. 2021, 333, 115950.
10. Huang, J.; Jones, A.; Waite, T.D.; Chen, Y.; Huang, X.; Rosso, K.M.; Kappler, A.; Mansor, M.; Tratnyek, P.G.; Zhang, H. Fe(II) Redox Chemistry in the Environment. Chem. Rev. 2021, 121, 8161–8233.
11. Kim, S.; Noh, J.Y.; Kim, K.Y.; Kim, J.H.; Kang, H.K.; Nam, S.; Kim, S.H.; Park, S.; Kim, C.; Kim, J. Salicylimine-Based Fluorescent Chemosensor for Aluminum Ions and Application to Bioimaging. Inorg. Chem. 2012, 51, 3597–3602.
12. Kumar, A.; Palfrey, H.A.; Pathak, R.; Kadowitz, P.J.; Gettys, T.W.; Murthy, S.N. The metabolism and significance of homocysteine in nutrition and health. Nutr. Metab. 2017, 14, 78.
13. Skovierova, H.; Vidomanova, E.; Mahmood, S.; Sopkova, J.; Drgova, A.; Cervenova, T.; Halasova, E.; Lehotsky, J. The Molecular and Cellular Effect of Homocysteine Metabolism Imbalance on Human Health. Int. J. Mol. Sci. 2016, 17, 1733.
14. Poole, L.B. The basics of thiols and cysteines in redox biology and chemistry. Free Radical Bio. Med. 2015, 80, 148–157.
15. Dao, N.V.; Ercole, F.; Urquhart, M.C.; Kaminskas, L.M.; Nowell, C.J.; Davis, T.P.; Sloan, E.K.; Whittaker, M.R.; Quinn, J.F. Trisulfide linked cholesteryl PEG conjugate attenuates intracellular ROS and collagen-1 production in a breast cancer co-culture model. Biomater. Sci. UK 2021, 9, 835–846.

16. Chen, X.; Wang, F.; Hyun, J.Y.; Wei, T.; Qiang, J.; Ren, X.; Shin, I.; Yoon, J. Recent progress in the development of fluorescent, luminescent and colorimetric probes for detection of reactive oxygen and nitrogen species. Chem. Soc. Rev. 2016, 45, 2976–3016.
17. Graves, D.B. The emerging role of reactive oxygen and nitrogen species in redox biology and some implications for plasma applications to medicine and biology. J. Phys. D Appl. Phys. 2012, 45, 263001.
18. Van-Nghia, N.; Ha, J.; Cho, M.; Li, H.; Swamy, K.M.K.; Yoon, J. Recent developments of BODIPY-based colorimetric and fluorescent probes for the detection of reactive oxygen/nitrogen species and cancer diagnosis. Coordin. Chem. Rev. 2021, 439, 213936.
19. Ogawa, M.; Takakura, H. In Vivo Molecular Imaging for Biomedical Analysis and Therapies. Anal. Sci. 2018, 34, 273–281.
20. Peng, F. Recent Advances in Cancer Imaging with (CuCl2)-Cu-64 PET/CT. Nucl. Med. Mol. Imaging. 2022, 56, 80–85.
21. Yan, Y.; Wang, H.; Zhao, Y. Radiolabeled peptide probe for tumor imaging. Chinese Chem. Lett. 2022, 33, 3361–3370.
22. Seetharam Bhat, K.R.; Samavedi, S.; Moschovas, M.C.; Onol, F.F.; Roof, S.; Rogers, T.; Patel, V.R.; Sivaraman, A. Magnetic resonance imaging-guided prostate biopsy—A review of literature. Asian J. Urol. 2021, 8, 105–116.
23. Kitada, N.; Maki, S.; Kim, S. Visible Light Bioluminescence Imaging Platform for Animal Cell Imaging. Methods Mol. Biol. 2022, 2524, 37–51.
24. Komatsu, H.; Kobayashi, E.; Gonzalez, N.; Rawson, J.; Ortiz, J.; Donohue, C.; Ku, H.T.; Kandeel, F.; Mullen, Y. Critical Considerations in Bioluminescence Imaging of Transplanted Islets Dynamic Signal Change in Early Posttransplant Phase and Signal Absorption by Tissues. Pancreas 2022, 51, 234–242.
25. Sato, K. Bioluminescence Imaging for Evaluation of Antitumor Effect In Vitro and In Vivo in Mice Xenografted Tumor Models. Methods Mol. Biol. 2022, 2524, 307–315.
26. Pan, X.; Gao, A.; Lin, Z. Fluorescence imaging of tumor immune contexture in immune checkpoint blockade therapy. Int. Immunopharmacol. 2022, 106, 108617.
27. Wu, X.; Li, H.; Lee, E.; Yoon, J. Sensors for In Situ Real-Time Fluorescence Imaging of Enzymes. Chem 2020, 6, 2893–2901.
28. Zhu, H.; Hamachi, I. Fluorescence imaging of drug target proteins using chemical probes. J. Pharm. Sci. 2020, 10, 426–433.
29. van Manen, L.; Handgraaf, H.J.M.; Diana, M.; Dijkstra, J.; Ishizawa, T.; Vahrmeijer, A.L.; Mieog, J.S.D. A practical guide for the use of indocyanine green and methylene blue in fluorescence-

guided abdominal surgery. J. Surg. Oncol. 2018, 118, 283–300.

30. Wang, J.; Li, C.; Jiang, G. Progress in Fluorescent Probes for Aminopeptidase N. Chem. Eur. J. 2018, 81, 972–980.
31. Xu, Y.; Liu, R.; Xu, K.; Dai, Z. Fluorescent Probes for Intraoperative Navigation. Prog. Chem. 2021, 33, 52–65.
32. Yagishita, A.; Ueno, T.; Tsuchihara, K.; Urano, Y. Amino BODIPY-Based Blue Fluorescent Probes for Aldehyde Dehydrogenase 1-Expressing Cells. Bioconjugate Chem. 2021, 32, 234–238.
33. Han, H.; Zhong, Y.; He, C.; Fu, L.; Huang, Q.; Kuang, Y.; Yi, X.; Zeng, W.; Zhong, H.; Yang, M. Recent advances in organic fluorescent probes for tumor related enzyme detection. Dyes Pigm. 2022, 204, 110386.
34. Pak, Y.L.; Swamy, K.; Yoon, J. Recent Progress in Fluorescent Imaging Probes. Sensors 2015, 15, 24374–24396.
35. Shaya, J.; Corridon, P.R.; Al-Omari, B.; Aoudi, A.; Shunnar, A.; Mohideen, M.I.H.; Qurashi, A.; Michel, B.Y.; Burger, A. Design, photophysical properties, and applications of fluorene-based fluorophores in two-photon fluorescence bioimaging: A review. J. Photoch. Photobio. C. 2022, 52, 100529.
36. Terai, T.; Nagano, T. Fluorescent probes for bioimaging applications. Curr. Opin. Chem. Biol. 2008, 12, 515–521.
37. Balleza, E.; Kim, J.M.; Cluzel, P. Systematic characterization of maturation time of fluorescent proteins in living cells. Nat. Methods 2018, 15, 47.
38. Han, Y.; Wang, X.; Li, S. Biocompatible Europium Doped Hydroxyapatite Nanoparticles as a Biological Fluorescent Probe. Curr. Nanosci. 2010, 6, 178–183.
39. Shore, A. A review on fluorescent inorganic nanoparticles for optical sensing applications (vol 6, pg 21624, 2016). RSC Adv. 2019, 9, 16565.
40. Wu, C.; Chiu, D.T. Highly Fluorescent Semiconducting Polymer Dots for Biology and Medicine. Angew. Chem. Int. Edit. 2013, 52, 3086–3109.
41. Zhang, J.; Huang, Y.; Wang, D.; Pollard, A.C.; Chen, Z.G.; Egap, E. Triblock near-infrared fluorescent polymer semiconductor nanoparticles for targeted imaging. J. Mater. Chem. C. 2017, 5, 5685–5692.
42. Chan, J.; Dodani, S.C.; Chang, C.J. Reaction-based small-molecule fluorescent probes for chemoselective bioimaging. Nat. Chem. 2012, 4, 973–984.
43. Gu, B.; Zhang, Q. Recent Advances on Functionalized Upconversion Nanoparticles for Detection of Small Molecules and Ions in Biosystems. Adv. Sci. 2018, 5, 1700609.

44. Berhanu, A.L.; Gaurav; Mohiuddin, I.; Malik, A.K.; Aulakh, J.S.; Kumar, V.; Kim, K. A review of the applications of Schiff bases as optical chemical sensors. TrAC, Trends Anal. Chem. 2019, 116, 74–91.
45. Immanuel David, C.; Prabakaran, G.; Nandhakumar, R. Recent approaches of 2HN derived fluorophores on recognition of Al3+ ions: A review for future outlook. Microchem. J. 2021, 169, 106590.
46. Zoubi, W.A. Biological Activities of Schiff Bases and Their Complexes: A Review of Recent Works. Int. J. Org. Chem. 2013, 3, 24.
47. Han, X.; Wang, Y.; Huang, Y.; Wang, X.; Choo, J.; Chen, L. Fluorescent probes for biomolecule detection under environmental stress. J. Hazard. Mater. 2022, 431, 128527.
48. Zhang, Y.; Hao, Y.; Ma, X.; Chen, S.; Xu, M. A dicyanoisophorone-based highly sensitive and selective near-infrared fluorescent probe for sensing thiophenol in water samples and living cells. Environ. Pollut. 2020, 265, 114958.
49. Lai, X.; Qiu, G.; Ye, Q.; Wang, R.; Liu, J. A reaction-based fluorescent probe for detecting o-phenylenediamine in water and lateritic soil samples. J. Photochem. Photobiol. A. 2020, 386, 112101.
50. Suratsawadee, A.; Wangmo, L.; Ratvijitvech, T.; Siripinyanond, A. A spoilage indicator card based on distance-based color change of paper impregnated with acid-base indicator for freshness monitoring of shrimp. Microchem. J. 2022, 175, 107110.
51. Zhong, K.; Zhou, S.; Yan, X.; Li, X.; Hou, S.; Cheng, L.; Gao, X.; Li, Y.; Tang, L. A simple H2S fluorescent probe with long wavelength emission: Application in water, wine, living cells and detection of H2S gas. Dyes Pigment. 2020, 174, 108049.
52. Choudhury, P.; Das, P.K. Progress and trends in self-assembly driven fluorescent organic nanoparticles: A brief overview. J. Indian Chem. Soc. 2021, 98, 100123.
53. Li, J.; Yim, D.; Jang, W.; Yoon, J. Recent progress in the design and applications of fluorescence probes containing crown ethers. Chem. Soc. Rev. 2017, 46, 2437–2458.
54. Liu, Z.; Zhou, X.; Miao, Y.; Hu, Y.; Kwon, N.; Wu, X.; Yoon, J. A Reversible Fluorescent Probe for Real-Time Quantitative Monitoring of Cellular Glutathione. Angew. Chem. Int. Edit. 2017, 56, 5812–5816.
55. Niu, L.; Chen, Y.; Zheng, H.; Wu, L.; Tung, C.; Yang, Q. Design strategies of fluorescent probes for selective detection among biothiols. Chem. Soc. Rev. 2015, 44, 6143–6160.
56. Park, S.; Kwon, N.; Lee, J.; Yoon, J.; Shin, I. Synthetic ratiometric fluorescent probes for detection of ions. Chem. Soc. Rev. 2020, 49, 143–179.

57. Wang, Y.; Zhang, L.; Han, X.; Zhang, L.; Wang, X.; Chen, L. Fluorescent probe for mercury ion imaging analysis: Strategies and applications. Chem. Eng. J. 2021, 406, 127166.
58. Zhang, J.; Wang, N.; Ji, X.; Tao, Y.; Wang, J.; Zhao, W. BODIPY-Based Fluorescent Probes for Biothiols. Chem.-Eur. J. 2020, 26, 4172–4192.
59. Fan, W.; Huang, X.; Shi, X.; Wang, Z.; Lu, Z.; Fan, C.; Bo, Q. A simple fluorescent probe for sensing cysteine over homocysteine and glutathione based on PET. Spectrochim. Acta A Mol. Biomol. Spectrosc. 2017, 173, 918–923.
60. Xu, K.; He, L.; Yang, Y.; Lin, W. A PET-based turn-on fluorescent probe for sensitive detection of thiols and H2S and its bioimaging application in living cells, tissues and zebrafish. New J. Chem. 2019, 43, 2865–2869.
61. Kumar, P.; Biswas, S.; Koner, A.L. Fast tyrosinase detection in early-stage melanoma with nanomolar sensitivity using a naphthalimide-based fluorescent read-out probe. New J. Chem. 2020, 44, 10771–10775.
62. Zhou, L.; Cui, J.; Yu, Z.; Zou, D.; Zhang, W.; Qian, J. A β-d-galactose-guided fluorescent probe for selectively bioimaging endogenous formaldehyde in living HepG-2 cells. Sens. Actuators B Chem. 2021, 332, 129494.
63. Xiong, K.; Huo, F.; Yin, C.; Yang, Y.; Chao, J.; Zhang, Y.; Xu, M. A off–on green fluorescent chemosensor for cyanide based on a hybrid coumarin–hemicyanine dye and its bioimaging. Sens. Actuators B Chem. 2015, 220, 822–828.
64. Gu, K.; Xu, Y.; Li, H.; Guo, Z.; Zhu, S.; Zhu, S.; Shi, P.; James, T.D.; Tian, H.; Zhu, W. Real-Time Tracking and In Vivo Visualization of β-Galactosidase Activity in Colorectal Tumor with a Ratiometric Near-Infrared Fluorescent Probe. J. Am. Chem. Soc. 2016, 138, 5334–5340.
65. Liu, F.; Wang, Z.; Wang, W.; Luo, J.; Kong, L. Red-Emitting Fluorescent Probe for Detection of γ-Glutamyltranspeptidase and Its Application of Real-Time Imaging under Oxidative Stress in Cells and in Vivo. Anal. Chem. 2018, 90, 7467–7473.
66. Cho, M.K.; Lim, C.S.; Sarkar, A.R.; Lee, H.W.; Choi, H.J.; Noh, C.; Shin, S.J.; Kim, H.M. A two-photon ratiometric probe for detection of hNQO1 enzyme activity in human colon tissue. Sens. Actuators Chem. 2018, 272, 203–210.
67. Shi, Y.; Huo, F.; Yin, C. Malononitrile as the ‘double-edged sword’ of passivation-activation regulating two ICT to highly sensitive and accurate ratiometric fluorescent detection for hypochlorous acid in biological system. Sens. Actuators Chem. 2020, 325, 128793.
68. Yu, H.; Fang, Y.; Wang, J.; Zhang, Q.; Chen, S.; Wang, K.; Hu, Z. Enhancing probe’s sensitivity for peroxynitrite through alkoxy modification of dicyanovinylchromene. Anal. Bioanal. Chem. 2022, 414, 6779–6789.

69. Wei, L.; Yi, L.; Song, F.; Wei, C.; Wang, B.; Xi, Z. FRET ratiometric probes reveal the chiral-sensitive cysteine-dependent H2S production and regulation in living cells. Sci. Rep. UK 2014, 4, 4521.
70. Zhang, H.; Liu, R.; Tan, Y.; Xie, W.H.; Lei, H.; Cheung, H.; Sun, H. A FRET-based Ratiometric Fluorescent Probe for Nitroxyl Detection in Living Cells. ACS Appl. Mater. Inter. 2015, 7, 5438–5443.
71. Aron, A.T.; Loehr, M.O.; Bogena, J.; Chang, C.J. An Endoperoxide Reactivity-Based FRET Probe for Ratiometric Fluorescence Imaging of Labile Iron Pools in Living Cells. J. Am. Chem. Soc. 2016, 138, 14338–14346.
72. Jia, X.; Chen, Q.; Yang, Y.; Tang, Y.; Wang, R.; Xu, Y.; Zhu, W.; Qian, X. FRET-Based Mito-Specific Fluorescent Probe for Ratiometric Detection and Imaging of Endogenous Peroxynitrite: Dyad of Cy3 and Cy5. J. Am. Chem. Soc. 2016, 138, 10778–10781.
73. Wei, X.; Hu, X.; Zhang, L.; Li, J.; Wang, J.; Wang, P.; Song, Z.; Zhang, J.; Yan, M.; Yu, J. Highly selective and sensitive FRET based ratiometric two-photon fluorescent probe for endogenous β-galactosidase detection in living cells and tissues. Microchem. J. 2020, 157, 105046.
74. Shen, Y.; Zhang, X.; Wu, Y.; Zhang, Y.; Liu, X.; Chen, Y.; Li, H.; Zhong, Y. A lysosome targetable fluorescent probe for palladium species detection base on an ESIPT phthalimide derivative. Spectrochim. Acta A Mol. Biomol. Spectrosc. 2018, 205, 66–71.
75. Zhou, X.; Liu, Y.; Liu, Q.; Yan, L.; Xue, M.; Yuan, W.; Shi, M.; Feng, W.; Xu, C.; Li, F. Point-of-care Ratiometric Fluorescence Imaging of Tissue for the Diagnosis of Ovarian Cancer. Theranostics 2019, 9, 4597–4607.
76. Ren, H.; Huo, F.; Wu, X.; Liu, X.; Yin, C. An ESIPT-induced NIR fluorescent probe to visualize mitochondrial sulfur dioxide during oxidative stress in vivo. Chem. Commun. 2021, 57, 655–658.
77. Jiang, G.; Zeng, G.; Zhu, W.; Li, Y.; Dong, X.; Zhang, G.; Fan, X.; Wang, J.; Wu, Y.; Tang, B.Z. A selective and light-up fluorescent probe for β-galactosidase activity detection and imaging in living cells based on an AIE tetraphenylethylene derivative. Chem. Commun. 2017, 53, 4505–4508.
78. Cheng, Y.; Dai, J.; Sun, C.; Liu, R.; Zhai, T.; Lou, X.; Xia, F. An Intracellular H2O2-Responsive AIEgen for the Peroxidase-Mediated Selective Imaging and Inhibition of Inflammatory Cells. Angew. Chem. Int. Ed. 2018, 57, 3123–3127.
79. Muthusamy, S.; Yin, S.; Rajalakshmi, K.; Meng, S.; Zhu, D.; Xie, M.; Xie, J.; Lodi, R.S.; Xu, Y. Development of a quinoline-derived turn-on fluorescent probe for real time detection of hydrazine and its applications in environment and bioimaging. Dyes Pigm. 2022, 206, 110618.
80. Gao, M.; Hu, Q.; Feng, G.; Tang, B.Z.; Liu, B. A fluorescent light-up probe with “AIE + ESIPT” characteristics for specific detection of lysosomal esterase. J. Mater. Chem. B. 2014, 2, 3438–3442.

81. Chen, X.; Xu, H.; Ma, S.; Tong, H.; Lou, K.; Wang, W. A simple two-photon turn-on fluorescent probe for the selective detection of cysteine based on a dual PeT/ICT mechanism. RSC Adv. 2018, 8, 13388–13392.
82. Yang, L.; Su, Y.; Geng, Y.; Zhang, Y.; Ren, X.; He, L.; Song, X. A Triple-Emission Fluorescent Probe for Discriminatory Detection of Cysteine/Homocysteine, Glutathione/Hydrogen Sulfide, and Thiophenol in Living Cells. ACS Sens. 2018, 3, 1863–1869.
83. Ning, Z.; Wu, S.; Liu, G.; Ji, Y.; Jia, L.; Niu, X.; Ma, R.; Zhang, Y.; Xing, G. Water-soluble AIE-Active Fluorescent Organic Nanoparticles: Design, Preparation and Application for Specific Detection of Cysteine over Homocysteine and Glutathione in Living Cells. Chem.-Asian J. 2019, 14, 2220–2224.
84. Yan, L.; Zhang, Y.; Xu, B.; Tian, W. Fluorescent nanoparticles based on AIE fluorogens for bioimaging. Nanoscale 2016, 8, 2471–2487.
85. Zhang, X.; Zhang, X.; Yang, B.; Zhang, Y.; Liu, M.; Liu, W.; Chen, Y.; Wei, Y. Fabrication of water-dispersible and biocompatible red fluorescent organic nanoparticles via PEGylation of aggregate induced emission enhancement dye and their cell imaging applications. Colloids Surf. B. 2014, 113, 435–441.
86. Zhang, Y.; Chang, K.; Xu, B.; Chen, J.; Yan, L.; Ma, S.; Wu, C.; Tian, W. Highly efficient near-infrared organic dots based on novel AEE fluorogen for specific cancer cell imaging. RSC Adv. 2015, 5, 36837–36844.
87. Zhao, Q.; Li, K.; Chen, S.; Qin, A.; Ding, D.; Zhang, S.; Liu, Y.; Liu, B.; Sun, J.Z.; Tang, B.Z. Aggregation-induced red-NIR emission organic nanoparticles as effective and photostable fluorescent probes for bioimaging. J. Mater. Chem. 2012, 22, 15128–15135.
88. Li, K.; Qin, W.; Ding, D.; Tomczak, N.; Geng, J.; Liu, R.; Liu, J.; Zhang, X.; Liu, H.; Liu, B. Photostable fluorescent organic dots with aggregation-induced emission (AIE dots) for noninvasive long-term cell tracing. Sci. Rep. UK. 2013, 24, 635–643.
89. Geng, J.; Zhu, Z.; Qin, W.; Ma, L.; Hu, Y.; Gurzadyan, G.G.; Tang, B.Z.; Liu, B. Near-infrared fluorescence amplified organic nanoparticles with aggregation-induced emission characteristics for in vivo imaging. Nanoscale 2014, 6, 939–945.
90. Feng, G.; Tay, C.Y.; Chui, Q.X.; Liu, R.; Tomczak, N.; Liu, J.; Tang, B.Z.; Leong, D.T.; Liu, B. Ultrabright organic dots with aggregation-induced emission characteristics for cell tracking. Biomaterials 2014, 35, 8669–8677.